On-site correlations in optical lattices: Band mixing to coupled quantum Hall puddles

Kaden R. A. Hazzard[*] and Erich J. Mueller

Laboratory of Atomic and Solid State Physics, Cornell University, Ithaca, New York 14853, USA
(Received 26 February 2009; revised manuscript received 2 January 2010; published 4 March 2010)

We extend the standard Bose-Hubbard model to capture arbitrarily strong on-site correlations. In addition to being important for quantitatively modeling experiments, for example, with rubidium atoms, these correlations must be included to describe more exotic situations. Two such examples are when the interactions are made large via a Feshbach resonance and when each site rotates rapidly, making a coupled array of quantum Hall puddles. Remarkably, even the mean field approximation to our model includes all on-site correlations. We describe how these on-site correlations manifest themselves in the system's global properties: modifying the phase diagram and depleting the condensate.

Optical lattice systems, where a dilute atomic gas is trapped in a periodic potential formed by interfering laser beams, provide a close connection between solid-state systems and atomic physics [1]. The models used to describe these systems generally assume that each lattice site's wave function is easily built up from single-particle states [2]. Here we argue that this approximation is inappropriate for quantitatively modeling current experiments and sometimes fails more drastically, for example, for resonant bosons. We show how to include arbitrary on-site correlations via a generalized Hubbard model, which can be approached by standard methods. By construction, the mean-field approximation to our model captures all on-site correlations, contrasting with prior approaches [3–8].

Our method's key idea is to first consider deep lattices, where lattice sites are isolated, and then solve the few-body problem on each site. Next, truncating to this few-body problem's low energy manifold, we calculate how tunneling couples the few-body states on neighboring sites. The resulting theory resembles a Hubbard model, but with number-dependent hopping and interaction parameters. We show that the corrections to the ordinary Bose-Hubbard model captured by this theory are crucial for quantitatively describing current rubidium experiments. They become even more important when the three-dimensional (3D) scattering length a becomes a significant fraction of the size of the Wannier states ℓ, such as in recent experiments on cesium atoms near a Feshbach resonance [9]. This approach is also essential for describing more exotic on-site correlations; as one example, one can rotate each lattice site, creating a lattice of coupled "quantum Hall puddles" [10,11]. Related ideas can be applied to double-well lattices and coupled "plaquettes" of four sites [12,13]. We explore the impact of the on-site physics on the extended system's phase diagram.

Our approach is most simply illustrated by a single-component Bose gas in a cubic sinusoidal lattice potential $V_p(x, y, z) = V_0 \sum_{\eta=x,y,z} \sin^2(\pi \eta/d)$ with the Hamiltonian

$$H_f = \int d^3 r \left\{ \psi^\dagger(r) \left[-\frac{\hbar^2}{2m} \nabla^2 - \mu + V_p(\mathbf{r}) \right] \psi(\mathbf{r}) + \frac{2\pi\hbar^2 a}{m} \psi^\dagger(\mathbf{r})\psi^\dagger(\mathbf{r})\psi(\mathbf{r})\psi(\mathbf{r}) \right\}, \quad (1)$$

*kh279@cornell.edu

where m is the particle mass, μ is the chemical potential, and ψ and $\psi^\dagger$ are bosonic annihilation and creation operators, respectively. Adding an additional trapping potential presents no additional difficulties.

Constructing the effective Hamiltonian. For each isolated site, we proceed to build up the many-body states from the solution of the n-body problem at site j: $\langle \mathbf{r_1}, \ldots, \mathbf{r_n} | \overline{|n\rangle}_j = \psi_n(\mathbf{r_1} - \mathbf{R_j}, \ldots, \mathbf{r_n} - \mathbf{R_j})$, which obeys $H_j \overline{|n\rangle}_j = \epsilon_n \overline{|n\rangle}_j$, where H_j is the same as Eq. (1)'s H_f, except replacing the periodic potential V_p there with an on-site potential V_j. A convenient approximation is to take $V_j(\mathbf{r}) = (m\omega^2/2)(\mathbf{r} - \mathbf{R_j})^2$, with $\omega = 2\sqrt{V_0 E_R}/\hbar$, the harmonic approximation to the site located at $\mathbf{R_j}$. For each site filling n, we restrict our on-site basis to the lowest-energy n-body state; however, including a finite number of excited states is straightforward. Note that even in the noninteracting case these states are *not* Wannier states. The principle difference is that states defined in this way are nonorthogonal. From these, however, one can construct a new set of orthogonal states $|n\rangle_j$, which hold similar physical meaning. In the noninteracting limit, the $|n\rangle_j$ approximate the Wannier states.

Because the single-site wave functions decay like Gaussians, it typically suffices to build up the effective Hamiltonian from neighboring sites. In particular, consider two sites, L and R, and the space spanned by $\overline{|n_L, n_R\rangle} = \overline{|n_L\rangle}_L \otimes \overline{|n_R\rangle}_R$, with overlaps $S^{(mn)} = \overline{\langle m, n|} \overline{|m+1, n-1\rangle}$. To lowest order in the overlaps, we can define orthogonal $|n_L, n_R\rangle$ by taking $|n_L, n_R\rangle = \overline{|n_L, n_R\rangle} - (1/2)[S^{(n_R, n_L)}\overline{|n_R + 1, n_L - 1\rangle} + S^{(n_L, n_R)}\overline{|n_R - 1, n_L + 1\rangle}]$.

Within this restricted basis, the effective Hamiltonian for these two sites is $H_{\text{eff}} = \sum_{n,m,n',m'} |n', m'\rangle\langle n', m'|H_f|n, m\rangle \langle n, m|$. Evaluation to lowest order in $S^{(mn)}$ yields on-site energy terms $\sum_{n,m}(E_n + E_m)|n, m\rangle\langle n, m|$ and a "hopping" term $-\sum_{nm} t^{(mn)}|m+1, n-1\rangle\langle m, n| + \text{H.c.}$, with

$$E_n = \overline{\langle n|}H_f\overline{|n\rangle},$$
$$t^{(mn)} = -\overline{\langle m+1, n-1|}H_f\overline{|m, n\rangle} + \frac{S^{(mn)}}{2}(E_m + E_n). \quad (2)$$

Additionally, there is an interaction term $U = \sum_{nm}[U_{\text{LL}}^{(n)} + U_{\text{RR}}^{(m)} + U_{\text{LR}}^{(n,m)}]|m, n\rangle\langle m, n|$, with $U_{\text{LL}}^{(m)} = U_{\text{RR}}^{(m)} = E_m$ and

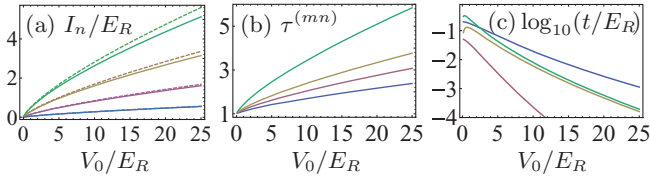$$U_{\text{LR}}^{(n,m)} = \overline{\langle m, n|}H_f\overline{|m, n\rangle} - E_m - E_n \quad (3)$$

FIG. 1. (Color online) (a) On-site energy with noninteracting energies subtracted off, $I_n = E_n - (3\hbar\omega/2 - \mu)n$, and energies scaled by $E_R = \hbar^2\pi^2/(2md^2)$, using typical ^{87}Rb parameters: lattice spacing $d = 532$ nm, scattering length $a = 5.32$ nm. Dashed curve, neglecting on-site correlations; solid curves, including correlations. Bottom to top curves: $n = 2, 3, 4, 5$, respectively. (b) Representative hopping matrix elements with on-site correlations, relative to those neglecting on-site correlations, $\tau^{(mn)} \equiv t^{(mn)}/[t\sqrt{(m+1)n}]$, as a function of lattice depth V_0 on a scale. Bottom to top lines: $t^{(03)}$, $t^{(31)}$, $t^{(05)}$, $t^{(35)}$, respectively. (c) For comparison, $t^{(01)}/E_R$ calculated from the exact Wannier states (top curve) along with our Gaussian approximation to it with and without nonorthogonality corrections (second- and third-highest curves, respectively). Also shown is the next-nearest-neighbor hopping matrix element (bottom curve). The effective Hamiltonian parameters are calculated perturbatively in a/d for a Gaussian ansatz.

to $O(S^2)$, consistent with the rest of our calculations. In the remainder of this article we will neglect the off-site interaction, Eq. (3), and the last term in Eq. (2). The former is rigorously justified as it falls off exponentially faster than the other interaction terms. Formally, the nonorthogonality contribution to Eq. (2) is suppressed only by a factor of $(V_0/E_R)^{1/4}$, with $E_R = \hbar^2\pi^2/(2md^2)$, but as shown in Fig. 1, it is typically small.

The simplest many-site Hamiltonian which reduces to this one in the limit of two sites is

$$H = -\sum_{\langle i,j \rangle; m,n} t_{ij}^{(mn)} |m+1\rangle_i |n-1\rangle_j \langle m|_i \langle n|_j$$
$$+ \sum_{i,n} E_n |n\rangle_i \langle n|_i, \qquad (4)$$

where $\sum_{\langle i,j \rangle}$ indicates a sum over nearest neighbors i and j. At higher order, one generates more terms such as next-nearest-neighbor hoppings, pair hoppings, and longer-range interactions.

Calculating the Hamiltonian parameters. Here we consider the cases of weak interactions, resonant interactions, and coupled quantum Hall puddles.

In the limit of weak interactions, one can estimate the parameters in Eq. (4) by taking the on-site wave function to be $\psi_n \propto \exp(-\sum_{j=1}^n r_j^2/2\sigma_n^2)$, with variational width σ_n. To leading order in a/d we find $E_n = E_R\{(3\sqrt{V_0/E_R} - \mu/E_R)n + (U/2)n(n-1)[1 - \frac{3\pi}{4\sqrt{2\pi}}(a/d)(n-1)(V_0/E_R)^{1/4}]\}$ with $U = (a/d)\sqrt{2\pi}(V_0/E_R)^{3/4}$ and $t^{(mn)} = t\sqrt{n(m+1)}[1 + \frac{\sqrt{2}a\pi^{5/2}}{4d}(m+n-1)(V_0/E_R)^{3/4}]$, with $t = V_0(\pi^2/4 - 1)e^{-(\pi^2/4)\sqrt{V_0/E_R}}$. Note that, as expected, interaction spreads out the Wannier functions, increasing the $t^{(mn)}$'s and decreasing the E_n's. Figure 1 shows several of the resulting $t^{(mn)}$'s as a function of V_0 for parameters in typical optical lattice experiments with ^{87}Rb. Also shown are $t^{(01)}$ and the next-nearest-neighbor hopping, t_{nnn}, calculated from

the exact Wannier states. Our estimates are consistent with previous work regarding t's n dependence [3–5], validating our approach. As can be seen in Fig. 1(c), the relative size of the next-nearest-neighbor hopping t_{nnn}/t is 10% (1%) for $V_0 = 3E_R$ ($V_0 = 10E_R$), justifying our approximation of including only nearest-neighbor overlaps to describe the system near the Mott state. Figure 1 also illustrates that the Gaussian approximation only qualitatively captures the behavior even for noninteracting particles. We also see that even for this weakly interacting case the number dependence of t is crucial for a quantitative description of the experiments. Similarly, the number dependence of the on-site interaction is quantitatively significant. This latter deficiency of the standard Hubbard model has been noted in the past, for example, by the MIT experimental group [14].

For more general experimental systems, one needs to include still more on-site correlations. As our first example, we consider lattice bosons near a Feshbach resonance [15,16], describing, for example, ongoing cesium atom experiments [9]. We restrict ourselves to site occupations $n = 0, 1, 2$, for which we have exact analytic solutions to the on-site problem for arbitrary a in terms of confluent hypergeometric functions [17]. Figure 2 shows graphs of E_n and $t^{(mn)}$ rescaled by $\hbar\omega$ as a function of a in the deep lattice limit.

As Fig. 2(b) illustrates dramatically, the hopping from and to doubly occupied sites is strongly suppressed near the Feshbach resonance when atoms occupy the lowest branch and is enhanced for the next-lowest branch. The former has implications for studies of boson pairing on a lattice [15,16], showing that one must dramatically modify previous models near resonance, and, as will be discussed more later in this article, the latter implies a substantial reduction of the $n = 2$ Mott lobe's size for repulsive bosons.

We give one further example, namely the case, similar to the one discussed in [10,11], where the individual sites of the optical lattice are elliptically deformed and rotated about their center. This is accomplished by rapidly modulating the
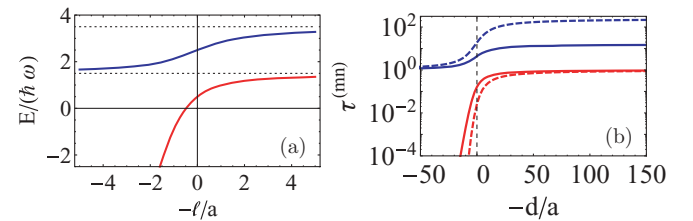

FIG. 2. (Color online) (a) On-site two-particle energy as a function of scattering length a rescaled by the on-site harmonic oscillator energy $\hbar\omega = 2\sqrt{V_0 E_R}$, for the two lowest-energy branches. The corresponding characteristic length is $\ell = \sqrt{\hbar/m\omega}$. (b) Log plot of rescaled hopping matrix elements $\tau^{(mn)} \equiv t^{(mn)}/[t\sqrt{(m+1)n}]$. Solid and dashed curves are $t^{(11)}/(\sqrt{2}t)$ and $t^{(12)}/(2t)$, respectively. We have chosen the lattice depth $V_0 = 15E_R$; this affects only the horizontal scale. In the ordinary Bose-Hubbard model, $t^{(mn)}/[\sqrt{(m+1)n}t] = 1$ for all m, n, as confirmed by this figure's $a = 0^-$ (lower, red) branch and $a = 0^+$ (upper, blue) branch limits. The resonance at $-d/a = 0$ separates the molecular side (a) from the atomic side (b). Note that $t^{(10)}/t$ (not shown) is universally equal to unity regardless of interaction strength, since interatomic correlations are absent when there is a single particle per site.

phase of the optical lattice lasers to generate an appropriate time-averaged optical potential. At an appropriate rotation speed Ω the lowest-energy n-particle state on each site is a $\nu = 2$ Laughlin state $\psi_n(\mathbf{r_1}, \ldots, \mathbf{r_n}) = \mathcal{N}_n[\prod_{i<j=1}^n (w_i - w_j)^2]e^{-\sum_j |w_j|^2/(4\ell^2)}$, where we define $w_j \equiv x_j + iy_j$, and $\mathcal{N}_n$ is a normalization factor with phase chosen to gauge away phase factors appearing in $t^{(mn)}$. Truncating to this set of states for $n = 0, 1, 2$, we produce an effective Hubbard model of the same form as Eq. (4). The hopping parameters for asymptotically deep lattices $V_0/E_R \gg 1$ are $t^{(01)} = t$, $t^{(02)} = t(\pi^2/32)(V_0/E_R)^{1/2}$, and $t^{(12)} = t(\pi^4/1024)(V_0/E_R)$, where $E_R = \hbar^2\pi^2/(2md^2)$ is the recoil energy, and t is the same as in the weakly interacting case treated earlier in this article; the interaction parameters are $E_m = \frac{\omega-\Omega}{2}m(m-1) - \mu m$. One particularly interesting aspect of this model of coupled quantum Hall puddles is that when the system is superfluid, the order parameter is exactly the quantity defined by Girvin and MacDonald [18,19] to describe the nonlocal order of a fractional quantum Hall state. Thus, when one probes the superfluid phase stiffness, one directly couples to this quantity.

Mean-field theory. The true strength of our approach is that the resulting generalized Hubbard model is amenable to all of the analysis used to study the standard Bose-Hubbard model. In particular, we can gain insight from a Gutzwiller mean-field theory (GMFT) [2,20]. This approximation to the ordinary Bose-Hubbard model gives moderate quantitative agreement with more sophisticated methods: For example, the unity site filling MI-SF transition on a 3D cubic lattice occurs at $(t/U)_c = 0.03408(2)$, while GMFT yields $(t/U)_c = 0.029$ [21].

In the ground state $|\Psi\rangle$, we introduce mean fields $\xi_m \equiv \langle\Psi|m+1\rangle\langle m|\Psi\rangle$. Neglecting terms which are quadratic in $\delta L_m^i = |i, m+1\rangle\langle i, m| - \xi_m$, the Hamiltonian is $H_{MF} = \sum_i H_{MF,i}$, with

$$H_{MF,i} = E_{n_i}|n\rangle_i\langle n|_i - z\sum_m[\zeta_m|m-1\rangle_i\langle m|_i$$
$$- \zeta_m\xi_{m-1} + \text{H.c.}], \quad (5)$$

where H.c. denotes Hermitian conjugate, z is the lattice coordination number, and $\zeta_n = \sum_m \xi_m t^{(mn)}$.

Truncating the number of atoms on a site to $n \leqslant n_{max}$, we self-consistently solve Eq. (5) by an iterative method. We start with trial mean fields, calculate the lowest-energy eigenvector of the $(n_{max} + 1) \times (n_{max} + 1)$ mean-field Hamiltonian matrix, then update the mean fields. We find that it typically suffices to take n_{max} roughly three times the mean occupation of the sites. Figure 3 illustrates how the density dependence of the parameters introduced by the on-site correlations modify the GMFT phase diagram—particularly the phase boundary's shape and the density and order parameter in the superfluid phase.

As one would expect, the topology of the MI-SF phase boundaries are similar to that of the standard Bose-Hubbard model, but the Mott lobes' shapes can be significantly distorted. Within mean-field theory the boundary's shape can be determined analytically by taking $|\Psi\rangle = \epsilon'|n-1\rangle + \sqrt{1 - \epsilon'^2 - \epsilon^2}f_{n-1}|n\rangle + \epsilon|n+1\rangle$ and expanding $\langle\Psi|H_{MF}|\Psi\rangle$ to quadratic order in ϵ and ϵ'. The Mott boundary corresponds to when the energy expectation value's Hessian changes sign;
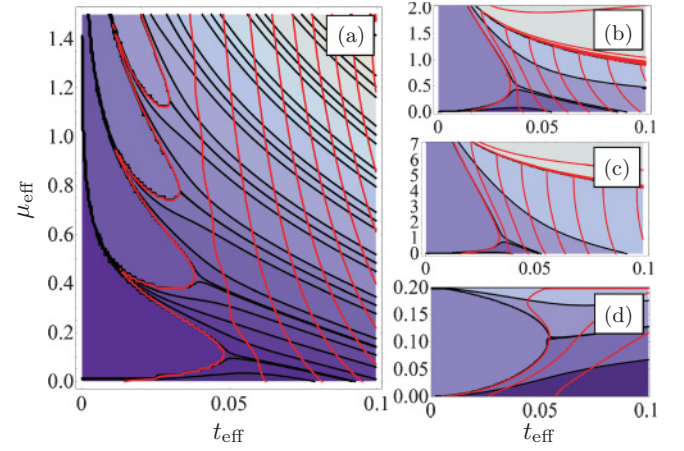

FIG. 3. (Color online) Representative Gutzwiller mean-field theory phase diagrams, showing constant density (black, roughly horizontal) and constant $\xi \equiv \zeta_1 + \zeta_2 + \zeta_3$ (red, roughly vertical) contours. ξ, similar to the condensate density, is a combination of the mean fields ζ_m, defined after Eq. (5). Density contours are $n = \{0.01, 0.2, 0.5, 0.8, 0.99, 1.01, 1.2, \ldots\}$ and order-parameter contours are $\xi = \{0.2, 0.4, \ldots\}$, except in (d), where we take contours $\xi = \{0.02, 0.04, \ldots\}$. The phase diagrams are functions of $\mu_{eff} \equiv \mu/E_R$ and $t_{eff} \equiv \exp(-\sqrt{V_0/E_R})$, where the lattice depth V_0 is the natural experimental control parameter. We plot versus t_{eff}, instead of V_0, as this is closer to the Hamiltonian matrix elements and more analogous to traditional visualizations of the Bose-Hubbard phase diagram. (a) Ordinary Bose-Hubbard model for $a = 0.01d$, (b) lattice bosons restricted to fillings $n = 0, 1, 2$ with $a = 0.01d$, on the next-to-lowest energy branch on the $a > 0$ side of resonance, (c) lattice boson model with $a = d$, and (d) fractional quantum Hall puddle array model, taking $\omega - \Omega = 0.1E_R$ (see text for details). Panels (b) and (c) use the Hamiltonian parameters from the exact two-particle harmonic well solution.

this boundary occurs when

$$[E_{n+1} - E_n + 2zt^{(n,n+1)}][E_{n-1} - E_n + 2zt^{(n-1,n)}]$$
$$= [zt^{(n,n)}]^2. \quad (6)$$

The five scaled parameters

$$\bar{\mu} \equiv \frac{E_n - E_{n-1}}{E_n}, \quad x_U \equiv \frac{E_{n+1} + E_{n-1} - 2E_n}{E_n},$$
$$\bar{t} \equiv \frac{t^{(n,n)}}{E_n}, \quad t^+ \equiv \frac{t^{(n,n+1)}}{t^{(n,n)}}, \quad t^- \equiv \frac{t^{(n-1,n)}}{t^{(n,n)}}, \quad (7)$$
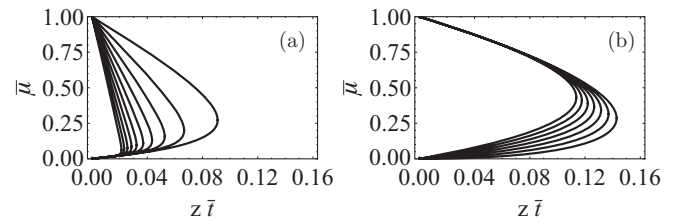

FIG. 4. Single lobe of the Mott-insulator–superfluid boundary. Complete characterization of the mean-field lobe shape in the $z\bar{t}$-$\bar{\mu}$ plane for all possible $t^\pm$'s [see Eq. (7) for definitions]. (a) Fix $t^- = 0.5$, vary t^+ from 1 (outer curve) to 21 (inner curve) in steps of 2. (b) Fix $t^+ = 1.5$, vary t^- from 0 (outer curve) to 1 (inner curve) in steps of 0.15.

completely characterize the shape of a filling-n Mott-phase boundary. Varying $\bar{t}$ and $\bar{\mu}$ while fixing the other parameters then maps out a Mott-lobe-like feature in the $\bar{t}$ and $\bar{\mu}$ plane, as illustrated in Fig. 4.

Summary and discussion. We have demonstrated an alternative approach to strongly correlated lattice boson problems. One constructs a model by truncating the on-site Hilbert space to a single state for each site filling n and includes only nearest-site, single-particle hoppings. While this approximation captures many multiband effects, it is not a multiband Hubbard model and in particular retains the ordinary Bose-Hubbard model's simplicity. In this method, arbitrary on-site correlations may be treated, even in the mean-field theory, and consequently it captures the condensate depletion, modified excitation spectra, altered condensate wave unction, and altered equation of state characteristic of strongly interacting bosons. We have calculated the mean-field Mott-insulator–superfluid phase boundary analytically and observables across the phase diagram numerically.

Finally, although we have truncated to a single many-body state for each filling n, no difficulty arises from including on-site many-body excitations in the Hamiltonian. These are especially important, for example, for double-well lattices and spinor bosons. The ideas also extend straightforwardly to fermions; see Refs. [22–26] for related considerations.

[1] I. Bloch, J. Dalibard, and W. Zwerger, Rev. Mod. Phys. **80**, 885 (2008).

[2] D. Jaksch, C. Bruder, J. I. Cirac, C. W. Gardiner, and P. Zoller, Phys. Rev. Lett. **81**, 3108 (1998).

[3] J. Li, Y. Yu, A. M. Dudarev, and Q. Niu, New J. Phys. **8**, 154 (2006).

[4] G. Mazzarella, S. M. Giampaolo, and F. Illuminati, Phys. Rev. A **73**, 013625 (2006).

[5] A. Smerzi and A. Trombettoni, Phys. Rev. A **68**, 023613 (2003).

[6] J. Larson, A. Collin, and J.-P. Martikainen, Phys. Rev. A **79**, 033603 (2009).

[7] O. E. Alon, A. I. Streltsov, and L. S. Cederbaum, Phys. Rev. Lett. **95**, 030405 (2005).

[8] P. R. Johnson, E. Tiesinga, J. V. Porto, and C. J. Williams, New J. Phys. **11**, 093022 (2009).

[9] Cheng Chin (private communication).

[10] M. Popp, B. Paredes, and J. I. Cirac, Phys. Rev. A **70**, 053612 (2004).

[11] S. K. Baur, K. R. A. Hazzard, and E. J. Mueller, Phys. Rev. A **78**, 061608(R) (2008).

[12] P. Barmettler *et al.*, Phys. Rev. A **78**, 012330 (2008).

[13] L. Jiang *et al.*, Phys. Rev. A **79**, 022309 (2009).

[14] G. K. Campbell *et al.*, Science **313**, 649 (2006).

[15] A. J. Daley, J. M. Taylor, S. Diehl, M. Baranov, and P. Zoller, Phys. Rev. Lett. **102**, 040402 (2009).

[16] D. B. M. Dickerscheid, U. Al Khawaja, D. van Oosten, and H. T. C. Stoof, Phys. Rev. A **71**, 043604 (2005).

[17] T. Busch, B.-G. Englert, K. Rzazewski, and M. Wilkens, Found. Phys. **28**, 549 (1998).

[18] S. M. Girvin and A. H. MacDonald, Phys. Rev. Lett. **58**, 1252 (1987).

[19] N. Read, Phys. Rev. Lett. **62**, 86 (1989).

[20] M. P. A. Fisher, P. B. Weichman, G. Grinstein, and D. S. Fisher, Phys. Rev. B **40**, 546 (1989).

[21] B. Capogrosso-Sansone, N. V. Prokof'ev, and B. V. Svistunov, Phys. Rev. B **75**, 134302 (2007).

[22] R. B. Diener and T.-L. Ho, Phys. Rev. Lett. **96**, 010402 (2006).

[23] H. Zhai and T.-L. Ho, Phys. Rev. Lett. **99**, 100402 (2007).

[24] M. Köhl, H. Moritz, T. Stoferle, K. Gunter, and T. Esslinger, Phys. Rev. Lett. **94**, 080403 (2005).

[25] L.-M. Duan, Phys. Rev. Lett. **95**, 243202 (2005).

[26] C. J. M. Mathy and D. A. Huse, Phys. Rev. A **79**, 063412 (2009).